345 E. 47 St., New York, N.Y. 10017

A Contribution to the Study of Exit Flow Angle in Radial Turbines

EDWARD A. BRIZUELA
Post Graduate Scholar
Department of Mechanical Engineering
Monash University
Melbourne, Australia

ABSTRACT

The emergence and evolution of relative whirling motions in the exducer region of an Inward Flow Radial Turbine is discussed. Existing models of relative motion are reviewed and expanded by consideration of the effect of centrifugal forces differences arising from velocity gradients. It is shown that the often observed phenomenon of outlet overturn/underturn is inherent to the use of straight-helix exducers.

Explicit mathematical relationships between exit velocities and radius are not available. If, however, such relationships could be considered linear, it is shown that two new reference radii may be identified such that the net outlet properties can be measured or computed at these locations as lump parameters. These radii are different from the often used hydraulic radius.

The new models and reference radii are verified using published experimental data.

NOMENCLATURE

A=Area (m^2) (normal to C_m)
a=Slope of V_m and C_m ($dimensionless$)
b=Slope of V_u ($dimensionless$)
c=Slope of C_u ($dimensionless$)
C=Absolute gas velocity (m/s)
h=Specific enthalpy (m^2/sec^2)
$\dot{m}$=Mass flow rate (kg/sec)
M=Mach number ($dimensionless$)
P=Total pressure (N/m^2)
R=Tip radius (m)
r=Hub radius; also generic radius (m)
T=Total temperature (K)
U=Rotor tangential velocity (m/sec)
V=Velocity of gas relative to the rotor (m/sec)

α=Angle between C and C_m
β_b=Angle between blade and C_m
β=Angle between V and C_m
Ω=Angular velocity (rad/sec)
ρ=Static density (kg/m^3)
τ=Torque ($N.m$)

Subscripts

h=hydraulic
m=meridional (on a plane containing the axis of rotation)
u=tangential (normal to m)
p=parallel to the blade surfaces
n=normal to p

Symbols

$\bar{}$=Average or net

INTRODUCTION

The exit flow angle from the rotor of an Inward Flow Radial Turbine (IFRT) determines the angular momentum of the efflux and hence the level of work generated by the machine.

At the design operating point the flow is initially assumed to leave the turbine on a perfectly axial direction (Whitfield(1990)). To achieve this the relative velocity is assumed uniform, and the blade trailing edge is given the shape of a straight helix, forming the exducer.

Experimental evidence (e.g., Hayami et al. (1990), Kofskey and Wasserbauer (1966)) shows that the exit flow angle in fact usually varies from hub to shroud and so do the axial and tangential components of absolute velocity. This being so, mass flow and torque should be computed as:

$$\dot{m} = \int_r^R \rho C_m \, dA \tag{1}$$

$$\tau = \int_r^R \rho r C_u C_m \, dA \tag{2}$$

For the experimenter this implies that two velocity traverses must be made. For the designer, the implication is that two laws

Presented at the International Gas Turbine and Aeroengine Congress and Exposition
Orlando, FL June 3-6, 1991

of radial variation of velocity must be assumed.

In the present work some of the reasons put forward for the radial variation of C_u and C_m are reviewed and added to. Further, it is shown that under certain conditions appropriate reference radii may be defined at which the outlet properties may be lumped or measured, and which only require measurement or assumption of one velocity gradient.

RELATIVE FLOW IN THE EXDUCER

Existing Models

Baines (1987) noted that measurements of relative velocity in the exducer area were not available in 1987. Although some researchers have reported to be working with this aim (e.g., University of Cincinnatti (1990)), experimental results are not available yet. Full viscous simulation of flow in IFRT's has not been reported either.

Inviscid numerical simulation has been presented by several authors (e.g. Mulloy and Weber (1982), Choo and Civinskas (1985)). A typical result is shown in Fig 1, adapted from the work of Molloy and Weber by addition of lines of circles which show average velocities between hub and shroud.

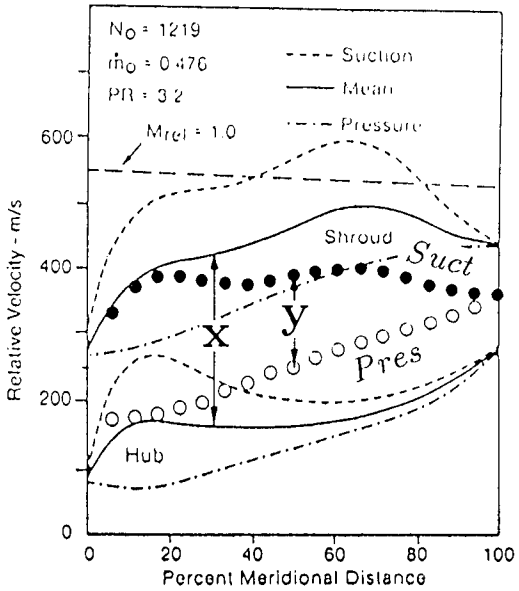

Meridional velocities
(Adapted from Ref [6])

Fig 1

The outlet flow is seen to possess higher velocity at the shroud than at the hub (plot (x)), and vanishing velocity difference on a blade-to-blade plane (plot (y)). The first effect is mainly due to the need to balance centrifugal forces in the axial-to-radial turn; the second is attributable to circulation around the trailing edge.

Further to this Baines (1987) has compiled models by various authors which add vortical motions generated by the gradient of centrifugal forces within boundary layers.

Regarding motion on a plane orthogonal to the flow, the relative whirl (of axial direction and magnitude $-\Omega$) is present at the entrance to the exducer. This will contribute a projected component near the outlet such that velocities V_n on the orthogonal plane are directed from pressure to suction face near the shroud, and *vice versa* at the hub. This is illustrated further in the following paragraph.

Additions to Existing Models

To these existing models we now add two further effects on the orthogonal plane. Firstly, referring to Fig 2, centrifugal forces will be generated at the radial-to-axial turn which are higher at the suction side than at the pressure side. This causes a rotation (indicated by $\mathcal{A}$ in the Figure) of the same sense of the relative whirl, which will also contribute a projected component. The counterrotating vortex discussed by Baines is also shown.

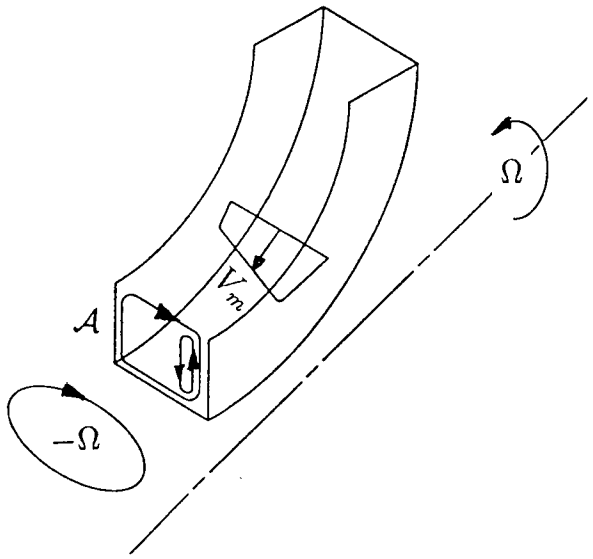

Whirls on the orthogonal plane

Fig 2

Secondly, referring to Fig 3, the higher shroud velocities will cause rotation of the sense indicated by the outer whirl $\mathcal{B}$ in the Figure. Again, the counterrotating vortex generated by the gradient of centrifugal forces within the boundary layer is also shown.

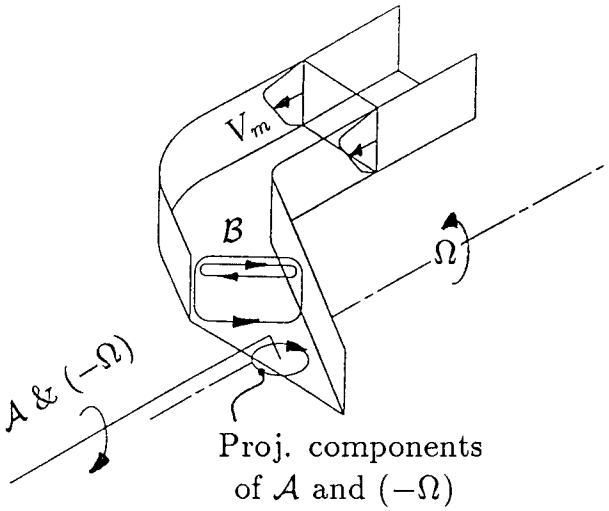

Proj. components
of $\mathcal{A}$ and $(-\Omega)$

Exit whirls

Fig 3

Whirl $\mathcal{B}$ is opposed to the projected components of the relative whirl and of whirl $\mathcal{A}$, and the balance of these whirls will influence the distribution of V_n.

At low fluid velocities both whirls $\mathcal{A}$ and $\mathcal{B}$ would be weak, and the component of relative whirl may predominate. At higher fluid velocities both whirls $\mathcal{A}$ and $\mathcal{B}$ will increase, but since only a fraction of $\mathcal{A}$ opposes $\mathcal{B}$, and since the exducer turn is often of smaller radius of curvature than the radial-to-axial turn, whirl $\mathcal{B}$ may predominate.

The results of Choo and Civinskas (1985), from where Fig 4 was adapted, show a case where whirl $\mathcal{B}$ prevails and rotation is reversed.

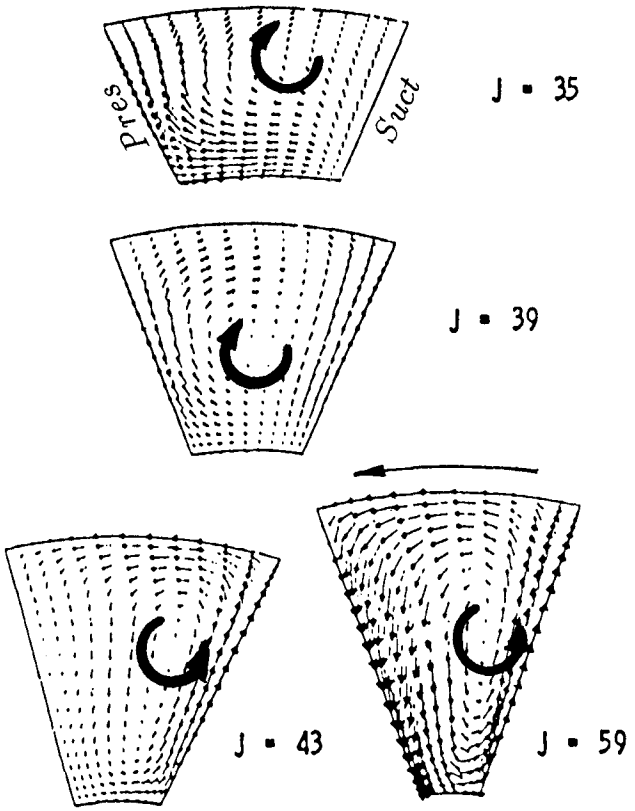

In-channel whirls
(Adapted from Ref [2])
Fig 4

The work of Choo and Civinskas applies to the turbine tested by McLallin and Haas (1980). This turbine produced approximately 16 kW at 35000 rpm, and relative air velocities were of the order of 200 m/sec. Fig 5 has been constructed using the test results, and the gradient of V_n is equivalent to a rotation of the same sense as the wheel motion, as found by Choo and Civinskas. Parallel velocity V_p increases from hub to shroud, and so does the exit axial velocity V_m (equal to C_m).

A turbine of similar dimensions but very lightly loaded (approximately 1 kW, air velocities of the order of 20 m/sec at the shroud and 15 m/sec at the hub) was tested by Hayami et al. (1990). Fig 6 corresponds to their data for 20 blades and 5000 rpm. The distribution of V_n shows that with such low velocities the relative whirl prevailed. Although the parallel component V_p is still slightly higher at the shroud, V_m now diminishes from hub to shroud.

To achieve a perfectly axial exit in the above cases a different manner of variation of blade angle with radius would have been required. Unfortunately, canted or curved trailing edges are undesirable from a structural point of view. Hence, radially varying axial and tangential velocities must be accepted as inherent to the use of radially straight blades in the presence of swirling flows.

Note however that if the tangential component C_u varies as in Figs 5 and 6, i.e, showing both underturn and overturn, the *net* angular momentum may be very small or even nil.

REFERENCE RADII

The above discussion indicates that the outlet flow is too complex for the axial and tangential velocities to be assigned a mathematical model with the current level of knowledge. The following assumes linear velocity variations, an assumption which, although supported by the results of McLallin and Haas (1980) and, to a certain extent, those of Hayami et al. (1990), is not based on a flow model.

It is desired to determine two radii, r_m and r_u, at which the net outlet mass flow and angular momentum may be lumped during design or measured during test.

Mass Flow Reference Radius

A linear variation of C_m may be expressed as:

$$C_m = \overline{C_m}\left[1 + a(\frac{r}{r_m} - 1)\right] \tag{3}$$

At $r = r_m$ the axial velocity is $\overline{C_m}$. We then equate:

$$\dot{m} = \overline{\rho C_m} A = \int_r^R \rho C_m \, dA \tag{4}$$

Assuming that the *radial* variation of static density is negligible, and with $dA = 2\pi r \, dr$, we obtain:

$$r_m = \frac{2}{3}\left(\frac{R^3 - r^3}{R^2 - r^2}\right) \tag{5}$$

This expression does not contain a; i.e., if C_m varies linearly, knowledge or assumption of the slope is not required.

Note that the appropriate radius is neither the hydraulic or rms radius $r_h (= \sqrt{(R^2 + r^2)/2})$ nor the average radius $\overline{r}$ $(= (R + r)/2)$. In fact :

$$\overline{r} \leq r_m \leq r_h \tag{6}$$

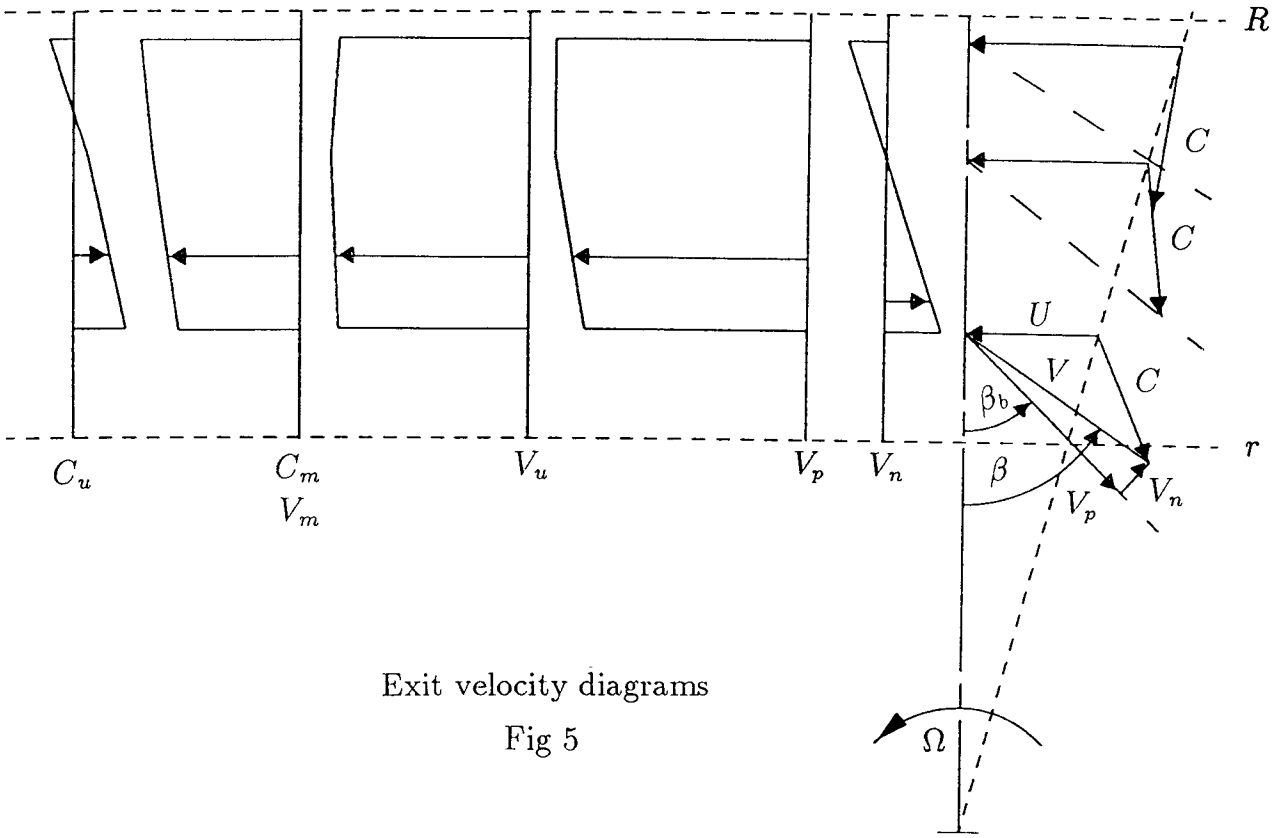

Exit velocity diagrams

Fig 5

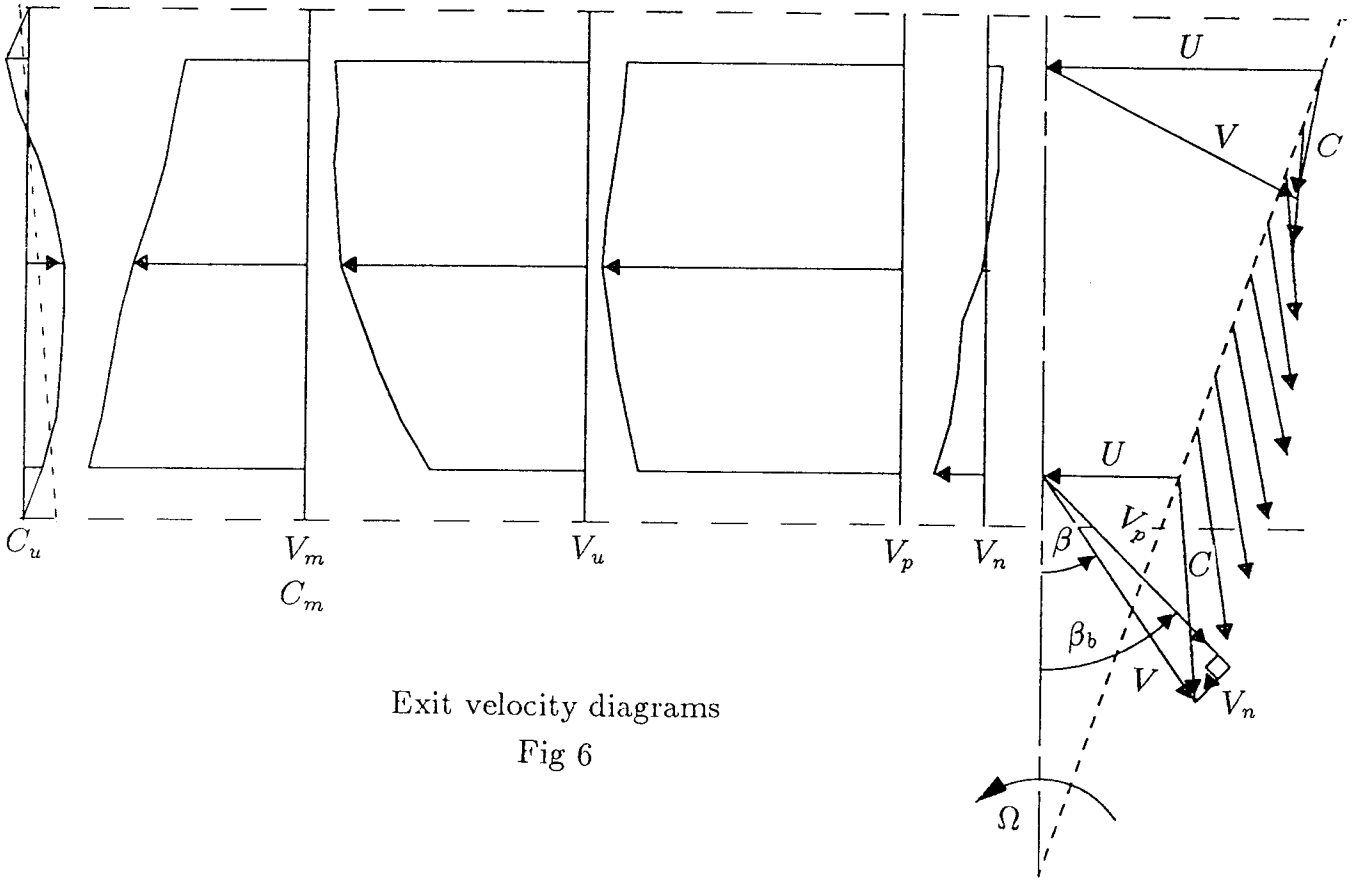

Exit velocity diagrams

Fig 6

Momentum Reference Radius

The reference radius r_u may be found by computing the change in outlet angular momentum:

$$\tau = \frac{\dot{m}}{\Omega}\overline{UC_u} = \int_r^R \frac{UC_u\, d\dot{m}}{\Omega} \tag{7}$$

As before, $\dot{m} = \overline{\rho}\overline{C_m}A$, and $\rho \simeq \overline{\rho}$. The mean wheel velocity is measured at r_u:

$$\overline{U} = \Omega r_u \tag{8}$$

A linear variation of V_u may be expressed as:

$$V_u = \overline{V_u}\left[1 + b(\frac{r}{r_u} - 1)\right] \tag{9}$$

Since $C_u = U - V_u$ (whence $\overline{C_u} = \overline{U} - \overline{V_u}$), it results:

$$C_u = \overline{C_u}\left[1 + \frac{\overline{U} - \overline{V_u}b}{\overline{C_u}}(\frac{r}{r_u} - 1)\right] \tag{10}$$

$$C_u = \overline{C_u}\left[1 + c(\frac{r}{r_u} - 1)\right] \tag{11}$$

To expand on the meaning of r_u, if at that point it is $V_u = U$, then the *net* angular momentum is zero ($\overline{C_u} = 0$). If, in addition, it is $b = 1$, then it is $C_u = 0$ *everywhere*. Note that $b = 1$ implies that the gradient of V_u be exactly Ω. The models and examples previously discussed show that this will generally not be the case. This again indicates that the exit flow will not be perfectly axial.

Integration yields an implicit equation for r_u:

$$r_u = \frac{2}{5}\frac{R^5 - r^5}{R^2 - r^2}\frac{a}{r_m}\frac{c}{r_u} + r_h^2\left[\frac{c(1-a)}{r_u} + \frac{a(1-c)}{r_m}\right] + r_m(1-c)(1-a) \tag{12}$$

Again, two gradients (a and c) or velocity traverses must be assumed or made.

If, however, the design net torque is zero ($\overline{C_u} = 0$), this reduces to:

$$r_u = \frac{\frac{2(R^5 - r^5)}{5(R^2 - r^2)}\frac{a}{r_m} + r_h^2(1-a)}{r_h^2\frac{a}{r_m} + r_m(1-a)}, \tag{13}$$

and only one gradient (a) is needed.

Note that the appropriate radius is not r_h; even if C_m is uniform ($a = 0$), the appropriate radius would be:

$$r_u = \frac{3}{4}\left(\frac{R^4 - r^4}{R^3 - r^3}\right), \text{ and now} \tag{14}$$

$$\overline{r} \le r_h \le r_u \tag{15}$$

Comparison with published test data

In the case of McLallin and Haas (1980) test data were:

$T_1 = 288.2\ K$
$P_1 = 94918\ N/m^2$
$\alpha_1 = 16.4$ deg
$\Omega = 3294.06\ rad/sec$
$P_2 = 31172\ N/m^2$
$T_2 = 223.5\ K$
$\dot{m} = 0.2372\ kg/sec$
$\Delta h = 65300\ m^2/sec^2$
$R_2 = 0.04719\ m$
$r_2 = 0.02286\ m$
$r_1 = 0.0752\ m$

C_{m2}	C_{u2}	r
$82.70\ m/sec$	$-41.96\ m/sec$	$0.0289\ m$
$112.11\ m/sec$	$13.96\ m/sec$	$0.0453\ m$

The upstream station radius is estimated from the figures in Ref [5] at 0.0777 m.

Using geometric and compressible flow relations we obtain:

$M_1 = 0.85$
$C_{u1} = 259.4\ m/sec$
$U_1 = 247.71\ m/sec$
$U_1C_{u1} = 64256\ m^2/sec^2$
$M_2 = 0.310$
$\rho_2 = 0.4632\ kg/m^3$
$A_2 = 5.3539\text{x}10^{-3}\ m^2$
$r_h = 0.03707\ m$

Regarding mass flow, application of the new formulae yields:

$r_m = 0.03643\ m$
$\overline{C_{m2}} = 96.17\ m/sec$
$a = 0.6777$

Then, the computed mass flow rate is:

$$\dot{m} = \overline{\rho_2}\overline{C_{m2}}A_2 = 0.2385\ kg/sec$$

This compares with the test value of 0.2372 kg/sec.

For angular momentum, the new formulae yield:

$r_u = 0.03862\ m\ (> r_h)$
$c = -14.73$
$\overline{C_{u2}} = -8.92\ m/sec$
$\overline{U_2} = 127.19\ m/sec$
$\overline{U_2}\ \overline{C_{u2}} = -1134.0\ m^2/sec^2$

Then, the computed specific enthalpy drop is:

$$\Delta h = U_1C_{u1} - \overline{U_2}\ \overline{C_{u2}} = 65390\ m^2/sec^2$$

The test value was 65300 m^2/sec^2.

The distributions of C_{u2} and C_{m2} are quite linear and thus the computed mass flow rate and specific enthalpy drop are only 0.5% and 0.14% respectively above the test values.

Similar results in respect to mass flow might be expected from the test data of Hayami et al. (1990), since the distribution of C_{m2} is also quite linear. The distribution of C_{u2} departs considerably from linearity, and similar results regarding specific enthalpy might not be achieved. It should be noted however that Hayami's test data were obtained under what can hardly be considered typical operating conditions for an IFRT.

The following test data may be deduced from the work of Hayami et al. (1990) at 5000 rpm:

$T_1 = 288.15\ K$
$P_1 = 101176\ N/m^2$
$\alpha_1 = 21.9$ deg
$\Omega = 523.6\ rad/sec$
$P_2 = 97393\ N/m^2$
$T_2 = 285.03\ K$

$\dot{m} = 0.335\ kg/sec$
$\Delta h = 3135.2\ m^2/sec^2$
$R_2 = 0.074\ m$
$r_2 = 0.030\ m$
$r_1 = 0.105\ m$

C_{m2}	r
$14.53\ m/sec$	$0.074\ m$
$30.77\ m/sec$	$0.030\ m$

Using geometric and compressible flow relations we obtain:

$M_1 = 0.179$
$C_{u1} = 56.33\ m/sec$
$U_1 = 54.98\ m/sec$
$M_2 = 0.093$
$\rho_2 = 1.1852\ kg/m^3$
$r_h = 0.05646\ m$

The exit free flow area is estimated from the figures to comprise 94% of the geometric area; hence:

$$A_2 = 1.3513\text{x}10^{-2}\ m^2$$

Regarding mass flow, application of the new formulae yields:

$r_m = 0.0551\ m$
$\overline{C_{m2}} = 21.50\ m/sec$
$a = -0.9458$

Then, the computed mass flow rate is:

$$\dot{m} = \overline{\rho_2}\,\overline{C_{m2}} A_2 = 0.344\ kg/sec$$

This compares with the test value of $0.335\ kg/sec \pm 5\%$.

Regarding angular momentum, there is no physical basis to justify approximating the test data by a linear distribution. It may be of interest, however, to compare both.

Good agreement in angular momentum may be obtained using a linear distribution with:

$r_u = 0.05603\ m\ (< r_h)$
$c = -6.2023$

This yields:

$\overline{C_{u2}} = -1.1337\ m/sec$
$\overline{U_2} = 29.3373\ m/sec$
$\overline{U_2}\ \overline{C_{u2}} = -33.26\ m^2/sec^2$

Then, the computed specific enthalpy drop is:

$$\Delta h = U_1 C_{u1} - \overline{U_2}\ \overline{C_{u2}} = 3130.0\ m^2/sec^2$$

The test value was $3135.2\ m^2/sec^2$.

The assumed linear distribution of C_u is shown in Fig 6 in dotted line over the experimental plot of C_u; it may be viewed as a coarse but not unreasonable approximation.

DISCUSSION AND CONCLUSIONS

Whirls on the orthogonal plane near the exit due to differences in centrifugal forces have been added to existing models. The resulting outlet flow is thus seen to comprise velocities parallel to the channel walls which increase from hub to shroud and are substantially uniform from blade to blade, plus velocities normal to the channel walls which correspond to rotations of a sense determined by geometry and operating conditions.

The use of straight helix exducers then leads to the often observed pattern of over/underturning. This, however, need not imply a nonzero outlet angular momentum.

A mathematical model for the outlet velocities is not available. If such model could be considered approximately linear with radius (and there is some experimental support for this), then the outlet mass flow rate may be computed using the axial velocity measured at a radius:

$$r_m = \frac{2}{3}\left(\frac{R^3 - r^3}{R^2 - r^2}\right) \tag{16}$$

This radius is larger than the mid-radius but smaller than the hydraulic or rms radius.

Further, if the desired net outlet angular momentum is zero, the exit flow angle must be zero at a radius:

$$r_u = \frac{\frac{2(R^5 - r^5)}{5(R^2 - r^2)}\frac{a}{r_m} + r_h^2(1-a)}{r_h^2\frac{a}{r_m} + r_m(1-a)} \tag{17}$$

To determine this radius only the slope of axial velocity C_m need be assumed or known. This radius is not equal to, and may be larger than, the hydraulic radius.

REFERENCES

1. BAINES, N. C.; "The aerodynamic design of radial-inflow turbines for compressible flow"; TPS/87.001, Imperial college of Science and Technology, Dept. of Mech. Eng., Thermal Power Section, London, January 1987.

2. CHOO, Y. K.; and CIVINSKAS, K. C.; "Three-dimensional inviscid analysis of radial turbine flow and a limited comparison with experimental data"; NASA TM-87091, November 1985.

3. HAYAMI, H.; SENOO, Y.; HYUN, Y. I.; and YAMAGUCHI, M.; "Effects of tip clearance of nozzle vanes on Performance of Radial Turbine Rotor"; in *Trans ASME, Journal of Turbomachinery*, Vol 112, Page 58, January 1990.

4. KOFSKEY, M. G., and WASSERBAUER, C. A.; "Experimental performance evaluation of a radial-inflow turbine over a range of specific speeds"; NASA TN-D-3742, November 1966.

5. McLALLIN, K. L.; and HAAS, J. E.;"Experimental performance and analysis of 15.04-centimetre tip diameter radial-inflow turbine with work factor of 1.126 and thick blading"; NASA TP-1730, October 1980.

6. MULLOY, J. M.; and WEBER, H. G.; "A radial inflow turbine impeller of improved off-design performance"; ASME Paper No. 82-GT-101, 1982.

7. UNIVERSITY OF CINCINNATTI Report, in *1990 International Gas Turbine and Aeroengine Technology Report*, International Gas Turbine Institute, ASME.

8. WHITFIELD, A.; "The preliminary design of radial inflow turbines"; in *Trans ASME, Journal of Turbomachinery*, Vol 112, Page 50, January 1990.